Journal of Engineering Physics and Thermophysics, Vol. 78, No. 6, 2005

COMPARATIVE ANALYSIS OF THE CALCULATION DATA ON AN UNSTEADY FLOW AROUND A CIRCULAR CYLINDER OBTAINED USING THE VP2/3 AND FLUENT PACKAGES AND THE SPALART–ALLMARAS AND MENTER TURBULENCE MODELS

S. A. Isaev,[a] P. A. Baranov,[a] N. A. Kudryavtsev,[a] D. A. Lysenko,[a] and A. E. Usachev[b]

UDC 532.517.2:4

An unsteady flow around a transversal circular cylinder has been analyzed on the basis of solution of Navier–Stokes and Reynolds equations, closed, in the latter case, using one- and two-parameter differential models of turbulence, by the implicit factorized method with the use of different-density structured and nonstructured grids. Solvers of specialized multiblock and universal packages have been tested.

Introduction. Modern computational technologies for solving various thermophysical and aerohydrodynamical problems are characterized by the following factors: a) packages are used at the industrial stage of numerical simulation, b) calculations are paralleled with the use of multiprocessors, which is considered as the most economical way of increasing the computational efficiency, and c) different-scale problems are represented on multiblock grids, which is considered as the most rational method of solving such problems [1]. In the present numerical investigation, we considered the genesis of multiblock computational technologies [2] based on solution of Navier–Stokes and Reynolds equations by the factorized implicit method on a set of intersecting different-scale grids, including sliding ones, used for solving the classical problems on unsteady laminar and turbulent flows around a circular cylinder. Prominence was given to the comparative analysis of the specialized package VP2/3, developed on the basis of multiblock computational technologies, with the known universal package FLUENT [3]. Estimation of the acceptability of two semiempirical models of turbulence — the one parameter Spalart–Allmaras model of eddy viscosity (SA) [4] and the two-parameter Menter zonal model of shear-stress transfer (MSST) [5] — has also been the subject of the present investigation.

As is known, the progress made in computational hydrodynamics in the last few decades is comparable to the progress made in the classical sciences over several centuries. These advances resulted from the rapid development of computational engineering; mathematical models of turbulence, combustion, radiative heat exchange, and others; and efficient numerical methods. Comparatively recently (in the lifetime of one generation — in the late 1960s–early 1970s), application programs written in one of the algorithmic programming languages (ALGOL or FORTRAN most often) served as the information basis of calculations. These programs were activated in large (BESM6 or CDC7600) computers in centers of collective use, and the results obtained were processed practically by hand.

Today, at the industrial stage of development of computational hydrodynamics [6], application programs comprise universal and specialized packages representing complex multicomponent intelligence systems written, as a rule, in object-oriented programming languages and having a "triad" structure: grid generator–solver–graphic data interpreter. A package involves catalogs of mathematical models and data of controlling physical processes, from elements of which a desired problem is formed. Packages are developed for definite computers — usually personal computers most often, but with a large random-access memory (512 Mb or larger). The widespread use of personal computers has made packages accessible to tens of thousands of users throughout the world. In recent years, the number of multiprocessor computers, in which parallel versions of packages can be used, has increased. Among the most high-capacity ("heavy") packages, which are especially popular, are the universal packages Fluent, Star CD, and CFX. In Russia,

[a]St. Petersburg State University, 38 Pilotov Str., St. Petersburg, 196210, Russia; email: isaev@SI3612.spb.edu; [b]Branch of the Central Aerohydrodynamics Institute, 17 Radio Str., Moscow, 107005, Russia. Translated from Inzhenerno-Fizicheskii Zhurnal, Vol. 78, No. 6, pp. 148–162, November–December, 2005. Original article submitted May 10, 2004.

1062-0125/05/7806-1199

prominence is given to specialized packages. Among these packages, the packages Flow Vision, SINF-2, and VP2/3 (velocity–pressure, two-dimensional and three-dimensional versions) stand out; they have characteristics approaching the characteristics of universal packages.

Many design and operation problems have been solved with the use of packages. However, the time it takes for complex problems to be solved measures several weeks or even months, which substantially limits the use of them in practice. A way out was found to a certain extent when computational operations were paralleled in multiprocessor (cluster) systems with the use of packages developed for this purpose. This allows one to increase the efficiency of solving application problems by many times. However, present-day multiprocessor complexes are very expensive, which has generated a need for the revival, after years, of centers of collective use, despite the fact that the Internet makes it possible to realize the practice of net calculations with the use of a remote terminal.

Unfortunately, the widespread use of packages creates the illusion that any problem can be solved on their basis. The producers of packages and the inexperience of purchasers (the majority of "heavy" packages are goods), thinking erroneously that packages can solve any of their problems and take the place of expensive physical experiments, may be a factor. What actually happens is that the available catalogs of mathematical models are far from being perfect and their data bases are not complete because there is ample room for further research on them. Moreover, the acceptability of mathematical models for solving complex problems has yet to be analyzed. The boundaries of application of most of the models are also not clearly understood. Thus, the most important problem of any numerical investigation is estimation of the adequacy of numerical forecasts. To do this estimation, it is necessary to test a package by solving a number of problems for which there are reliable experimental and calculation data. In all likelihood, one should select not a better or a proper package but an acceptable model and should master the modern computational methodology realized in a package, i.e., the case in point is the professional skill of estimators — specialists in the field of numerical hydrodynamics.

The experience in simulation of hydromechanical processes suggests that there is a need for estimating their different-scale structural features. To do this, it is necessary to know them apriori and select a computational grid that would allow one to represent them correctly. The latter circumstance explains, in many respects, the recent development of multiblock computational technologies involving the use of different-scale, structured, intersecting computational grids of simple topology. In 1996, it was proposed to calculate the problem on a laminar flow around a thick profile with vortex cells on the basis of intersecting structured grids of the ○ type; this concept was then realized in the computational complex VP2/3 [7]. At first, the indicated multiblock approach was developed for calculating steady turbulent flows with the use of the two-parameter dissipative Launder–Spalding model of turbulence. A large step toward increasing the quality of the numerical simulation of turbulent separation flows on intersecting multiblock grids was made when the model of shear-stress transfer was approved. This model was verified in the process of solving the problem on an air flow in plane-parallel and extending channels with a circular vortex cell on one of the walls [8, 9], the problem on a steady flow around a transversal cylinder with a separating plate [10], and the problem on the turbulent heat exchange in the neighborhood of a shallow spherical hole on a plane [11]. The problem on the oscillations of a physical pendulum in a cavity filled with an incompressible fluid was solved with the use of sliding grids [12]. Two multiblock complexes, which can be used in practice for numerical simulation of the smoke-screen of subway tunnels in the case of a fire in a car [13] and a dangerous shift of the wind in the vicinity of an airport, have been developed [14].

A Multiblock Computational Algorithm. An algorithm for numerical simulation of laminar and turbulent vortex flows of a viscous incompressible fluid in multiply connected curvilinear computational regions has been developed. The algorithm is based on solution of nonstationary Navier–Stokes and Reynolds equations by the finite-volume method of factorized global iterations within the framework of the concept of splitting by physical processes [7]. The core of the algorithm for solving the master equations written in increments of dependent variables in generalized curvilinear coordinates is a modified coordinated SIMPLEC procedure of pressure correction, used in each time step. The two-step predictor–corrector procedure is used for determining the increments of the Cartesian velocity components and the pressure. The convective terms in the explicit side of a pre-linearized system of initial equations for momentum and the characteristics of turbulence are approximated, respectively, by a QUICK one-dimensional upwind Leonard scheme with quadratic interpolation and a TVD scheme. The stability of the computational algorithm is provided by approximation of the convective terms on the implicit side of the transport equations by an upwind scheme with single

differences. The diffusion terms on both sides of the equations are traditionally represented by a scheme with central differences. For damping of the high-frequency oscillations, an additional artificial diffusion with a transport coefficient proportional to the kinematic viscosity is introduced into the diffusion terms on the implicit side of the equations. In the case where calculations are performed by a centered pattern, the pressure is corrected using a Rhie–Chow monotonizer (regulator) with an empirically determined factor of 0.1 [15]. And finally, the difference equations are solved by the method of incomplete matrix factorization in the Stoun version (SIP) [7, 15]. In the case where the procedure of global iterations is used for solving the momentum equations, one local iteration corresponds to several (as much as six) iterations in the unit of pressure correction and a small (as small as four) number of iterations in the unit for calculating the characteristics of turbulence.

According to [15], nonstationary processes are exactly defined by transport equations, the nonstationary term in the explicit side of which are approximated by the three-point Peire scheme of the second order of approximation with respect to time. However, it is good to use the implicit Euler scheme in the case where a small time step (of the order of 0.02) is selected.

As was noted above, the multiblock algorithm was developed for numerical simulation of vortex flows in multiply connected regions of bodies with vortex cells [7]. This algorithm allows one to decompose a computational region of complex geometry into fragments and, then, to perform calculations using intersecting grids of simple topology. In a number of works (see, e.g., [16, 17]), it was proposed to use this approach for estimating different-scale structural elements of a flow, such as boundary and shear layers, vortex streets, separation zones, and others. Thus, the approach proposed is similar, to a certain extent, to the use of grids adapted to the solution of a problem. It should be noted that the parameters in the region of intersection of grids can be determined by linear interpolation [7].

The global interactions in each time step are considered as completed when the fields of dependent variables converge with a definite acceptable accuracy [7, 15], for example, $5\cdot10^{-4}$ for increments of the velocity components and the pressure and $5\cdot10^{-5}$ for increments of the turbulence energy or the eddy viscosity. The relaxation coefficients used for calculating the increments of the Cartesian velocity components and for the pressure correction are assumed to be respectively 0.5 and 0.8.

Calculation of a Laminar Flow Around a Circular Cylinder. Methodical investigation of an unsteady laminar flow around a circular cylinder at a definite Reynolds number (Re = 140) was carried out for the purpose of reproduction, in a numerical experiment, of the physical conditions of visualization of a Kármán vortex street (presented in the known Van Dyke atlas of flows) by smoke [18]. A smoke jet introduced into an air flow passes around the circular cylinder and colors the vortex flow in the wake. This problem on a two-phase flow around a body is solved using the FLUENT package on a nonstructured triangular grid adopted to the CO concentration. At the same time, the interaction of a uniform flow of an incompressible viscous fluid, propagating with a velocity U, with a cylinder of diameter D (Fig. 1a) is calculated without regard for a smoke jet with the use of the VP2/3 package on structured multiblock circular and rectangular-cylindrical grids. The parameters U and D are used as characteristics. The Cartesian coordinate system x, y is introduced and is related to a given critical point of the cylinder.

The configuration of the region surrounding the cylinder with an outer boundary spaced by a large distance (30 calibers or 30 cylinder diameters in the present investigation) from the center has the form of a circle; this configuration was used in the majority of earlier investigations [7, 10, 15, 19–23]. Fixed boundary conditions, $u = 1$, $v = 0$, and $p = 0$, are set in the input left half the region. The so-called "soft" boundary conditions, under which the parameters of a flow at a boundary are determined by extrapolation (quadratic extrapolation in the present work) from the inner points adjacent to it, are set at the outer boundary. The adhesion conditions $u = v = 0$ are set on the cylinder surface around which a flow passes. The initial conditions, at the instant of time $t = 0$, correspond to the conditions of sudden stopping of the cylinder in a fluid flow, i.e., the input conditions are extended to the whole computational region.

For the purpose of methodical comparison of results and estimation of the adequacy of numerical forecasts, we considered an additional rectangular computational region (Fig. 1). It should be noted that a computational region of this configuration is considered as most appropriate for estimation of the characteristics of a far wake downstream of a cylinder within the framework of modern multiblock computational technologies [16, 24, 25]. The introduction of a special rectangular grid into the region downstream of a circular cylinder allows one to correctly estimate the large-scale vortices propagating in a Kármán street. The above-mentioned input conditions are set at the left boundary of the

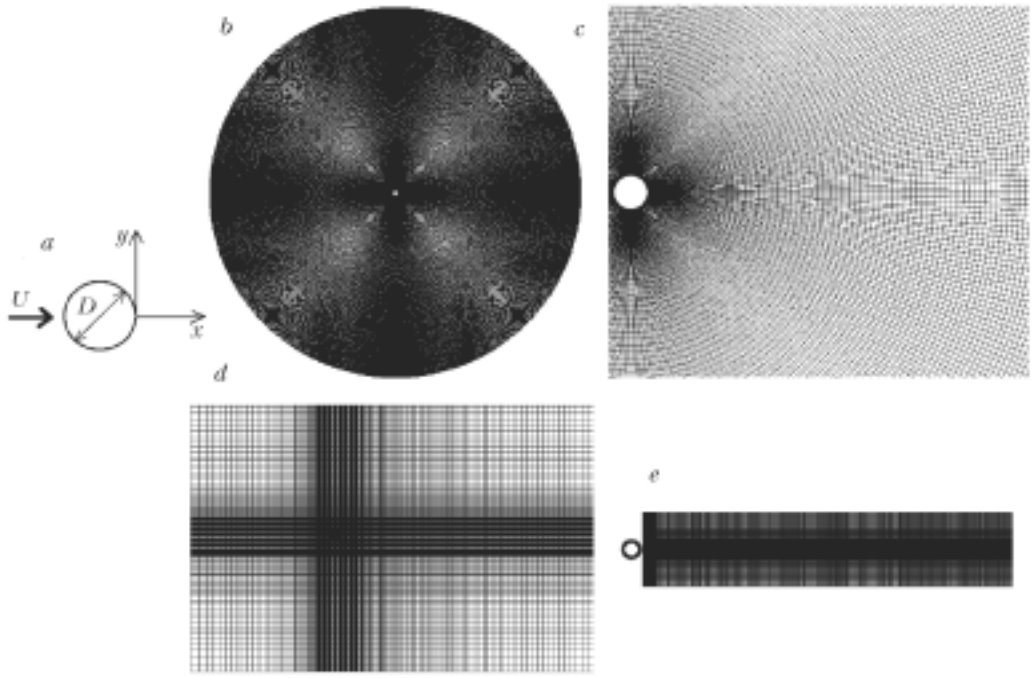

Fig. 1. Scheme of a flow around a cylinder (a) constructed using the VP2/3 package and structured multiblock computational grids of different type and scale: b, c) cylindrical grids; d, e) combined rectangular-cylindrical grids.

computational region and soft conditions are set at the other boundaries. The other conditions are similar to the above-described conditions set for the circular computational region.

Thus, we will analyze an unsteady laminar flow around a circular cylinder with the use of two multiblock grids: a multistage cylindrical grid (Fig. 1b and c) and a grid comprising a combination of different-scale rectangular and cylindrical grids (Fig. 1d and e).

The base multiblock cylindrical grid covers a circular computational region of radius 33.6 and includes three ring stages: 1) a layer of thickness 0.1, adjacent to the cylinder, is covered by a 15×120 grid with a near-wall pitch of 10^{-3}; 2) a zone of width 3 is covered by a 50×420 grid; 3) a ring zone of width 30 is covered by a 250×420 grid.

A rectangular computational region of length 49 and width 34, separated 17 from the input boundary, is covered by a grid containing 170×120 cells with a minimum step of 0.1 along both coordinates (Fig. 1d). A two-stage grid covers a region located near the circular cylinder: a 40×160 cylindrical grid with a near-wall step of $5 \cdot 10^{-4}$ covers a ring region of width 0.2 adjacent to the wall around which a flow passes; a ring of width 2 is covered by a grid containing 45×160 cells. For representation of the near and far wakes downstream of the cylinder, an additional rectangular grid containing 275×80 cells with a minimum pitch of 0.05 is introduced; it covers a subregion of length 27.5 and width 5.6 with an origin at the point $x = 0.3$.

Note that the grids covering ring subregions have a constant pitch along the peripheral coordinate, while the cylindrical grids covering regions located along the radial coordinate and all the rectangular grids are irregular with a bunching to the surface of the cylinder and in the wake downstream of it. In this case, the ratio between the neighboring pitches of the grids does not exceed 1.3.

The dimensionless time step Δt, determined in fractions of the ratio between the diameter of the cylinder and the characteristic velocity of the incoming flow, was estimated in earlier test calculations [7, 20, 23–25] at 0.02.

For comparison of different methods of solving the Navier–Stokes equations on grids of different topology with the use of different solvers, we performed calculations with the FLUENT package [3]. In this case, the variables used should have a dimension because the FLUENT package is universal in character and involves numerous dimension data bases.

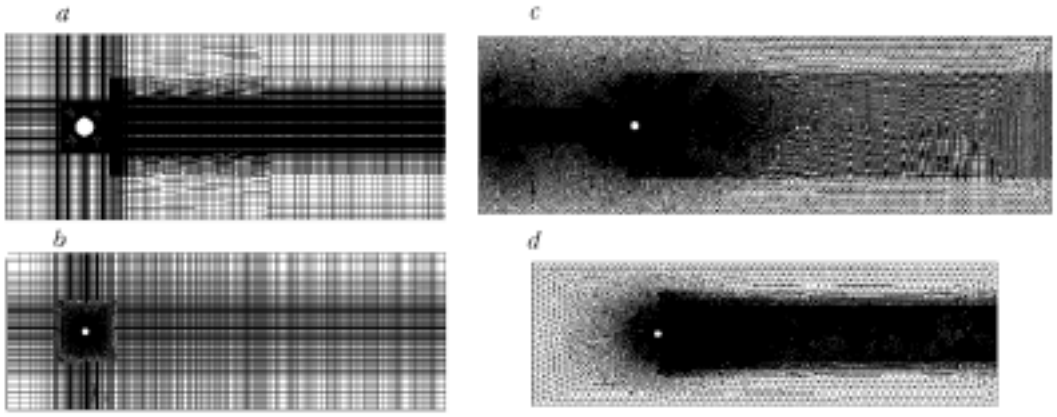

Fig. 2. Computational grids of different adaptation used in the FLUENT package: structured quadrangular canonical grids of types 1 (a) and 2 (b); nonstructured triangular grids of types 3 (c) and 4 (d).

The computational region represents a rectangle of size 6.5 × 2 m. A cylinder of diameter 0.1 m is located at a distance of 17.5 calibers from the input boundary and symmetrically relative to the upper and positioned boundaries. The width of the gas jet supplied is 0.01 m (10% of the cylinder diameter). The simulation is carried out with the use of a nonstructured triangular grid. The cylinder is surrounded by a structured ring grid with a minimum near-wall step of 10^{-5} m. The cylinder profile is divided into 100 equal intervals. The grid is adapted to three regions: 1) a circle of radius 0.5 m, the center of which coincides with the center of the cylinder; 2) a rectangular region of size 4.65 × 1.2 m, used for better representation of the wake formed downstream of the cylinder; 3) a rectangular region of size 1.75 × 0.4 m, used for better representation of the zone where the air flows are mixed with the smoke jet. The time step is taken to be equal to 0.1 sec.

A gas mixture of air with smoke contains O_2, N_2, and CO. The density of the mixture is calculated by the formula

$$\rho = 1 / \sum_i Y_i / \rho_i \, .$$

The viscosity of the mixture is determined in the following way:

$$\mu = \sum_i Y_i \mu_i \, ,$$

where Y_i is the mass fraction of the ith component.

The input boundary conditions are defined by the velocities of the flows and the mass fractions of the components (0.23 for O_2 and 1 for CO). The velocity of the incoming flow U is determined at a definite value of the Reynolds number (140). In this case, the density and viscosity of air are used (ρ = 1.225 kg/m^3, μ = 1.7894·10^{-5} kg/(m·sec)) and the cylinder diameter is taken to be D = 0.1 m. The symmetry conditions are set at the upper and lower boundaries of the computational region. "Soft" conditions are set at the output boundary.

A system of nonstationary Navier–Stokes equations [26], averaged, in the general case, according to Reynolds, and an equation for transport of gas-mixture components are solved by the factorized finite-difference method.

The computational algorithm involves the third-order approximation of the convective terms in equations by the QUICK scheme, the second-order approximation of the pressure, the PISO procedure of pressure correction, and the second-order discretization with respect to time by an implicit scheme [15, 27].

Figures 2 and 3 present computational grids with different levels of adaptation, constructed by the grid generator of the FLUENT package. The number of cells and triangular elements is as large as 500,000. Traditional [27] grids with quadrangular cells (Fig. 2a and b) and nonstructured grids with triangular cells (Fig. 2c and d) are considered. Particular emphasis is placed on the triangular grids (Fig. 3) adapted to the solution of the problem (the CO con-

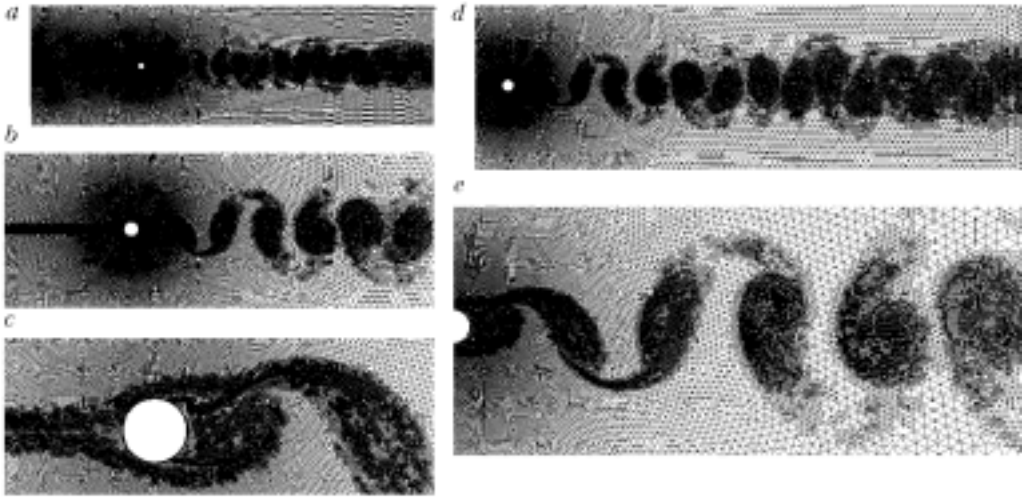

Fig. 3. Different-scale nonstructured triangular grids of type 5 with a gradient adaptation with respect to the CO concentration used in the FLUENT package.

TABLE 1. Influence of the Type of Grid on the Integral Force, Averaged, and Pulsating Characteristics of a Cylinder Determined Using Different Packages

Package	Type of grid	Characteristics of cylinders		
		$\overline{C_x}$	C_x'	Sh
VP2/3	Circular	1.29	0.0136	0.178
	Rectangular	1.30	0.0126	0.177
	Half-disk	0.9495	0	—
FLUENT	Rectangular	1.27	0.011	0.172

centration), because these grids are best suited for representation of details of the vortex structure of a flow around a cylinder. This is explained by the fact that the density of cells in them is larger where this is desired, i.e., in the zones of vortex cores. Nonetheless, despite the high accuracy of reproduction of the pattern of a flow and the minimum errors in the solution, only a grid containing an extremely large number of cells (as large as 1,500,000) can be adapted to a solution.

Some of the methodical results obtained are presented in Figs. 4–6 and in Table 1.

As is known (see, e.g., [7]), an unsteady laminar flow around a circular cylinder develops in several stages beginning with the state of sudden motion in a medium at rest (Fig. 4a and b).

The first stage represents the initial period of impact interaction of a flow with the cylinder, as a result of which a symmetric separation zone is formed in the near wake. It should be noted that the problem on a flow in this phase has long been used for testing computational methods used for numerical simulation [7], even though small (of the order of several units) time intervals were considered in this case. However, judging from the evolution of the maximum (in magnitude) velocity of a reverse flow, the initial phase can actually be divided into two periods: a very short time interval of duration several seconds, in which $|u_{\min}|$ reaches a maximum (about 70% of the incoming-flow velocity) and a fairly long (of the order of 40–60) interval of linear increase in $u_{\min}(t)$ to 0.2. The change in the minimum pressure with time correlates very well with the time dependence of the frontal resistance of the cylinder. In the initial time interval from 0 to 15, the characteristics C_x and $|p_{\min}|$ change very rapidly, and then they decrease gradually. It should be noted that $C_y = 0$ at the first stage, which is reasonable because an unsteady flow around a circular cylinder develops symmetrically. It follows from Table 1 that C_x, in the interval where it decreases gradually, approaches the drag coefficient of the cylinder in the case where a steady laminar flow passes around it. This coefficient was calculated for a flow in a semiplane and corresponds, to a certain extent, to an unsteady flow around a cylinder with a separating plate in the wake.

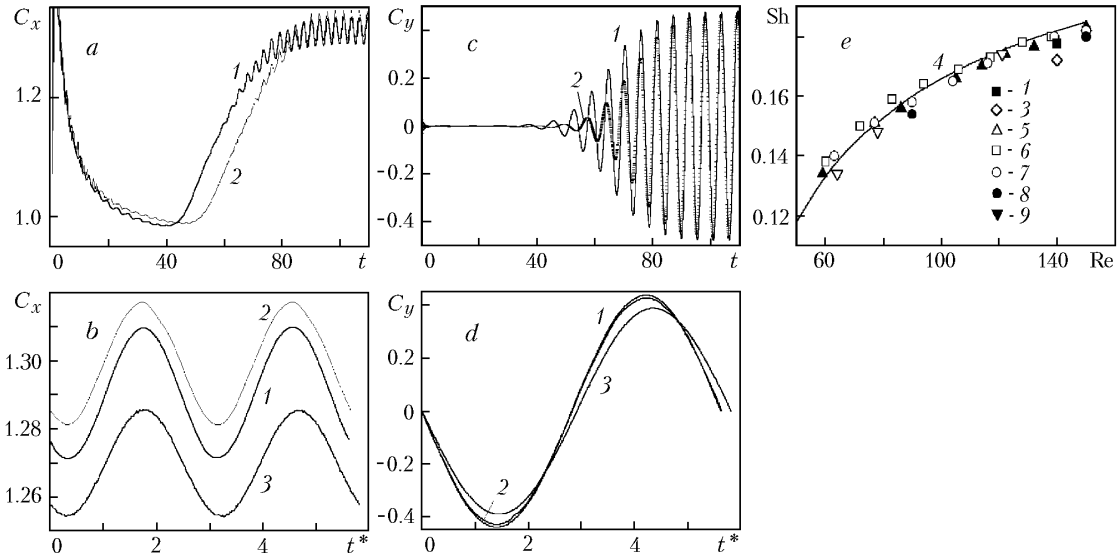

Fig. 4. Time evolution of the coefficients of frontal resistance (a, b) and transverse force (c, d) of a circular cylinder around which a viscous-fluid flow (Re = 140) passes calculated using circular (1) and rectangular (2) block grids and the VP2/3 package; curve 3 was obtained on the basis of the FLUENT package; e) comparison of the calculated (1, 3, 4, 8, 9) and experimental (5, 6, 7) dependences of the Strouhal number on the Re number: 4) [28], 5) [29], 6) [30], 7) [31], 8) [20], 9) [32]; t^* is the instant of time at which $C_y = 0$.

At the second stage of the transient process, the stability of the fluid motion in the vortex wake decreases. It is often explained by the fact that the flow responds to small perturbations occurring invariably in physical experiments and arising in calculations, e.g., due to the round-off errors, in particular when calculations are carried out with a single accuracy. On occasion such perturbations are specially introduced in the process of solving a problem to "drive" a vortex system. Note that our calculations did not reveal this necessity; a symmetric flow around the cylinder destabilized in the natural way and in an approximately identical manner for different grids.

The abrupt change in the behavior of the time dependences of the integral and extremum local parameters of a flow at $t > 40$, manifesting, first of all, a tendency toward a rapid increase in the rarefaction in the wake and an increase in the drag and in the transverse force, has engaged our attention. However, as follows from Fig. 4c, the asymmetry of the flow begins to develop in the far wake much earlier (at t of the order of 20–30). A transverse pulsating motion of the fluid in the geometric symmetry plane of the cylinder, arising at the right boundary of the computational region, gradually occupies a larger and a larger space and reaches the cylinder. It should be noted that the velocity and pressure pulsations generated in the far wake are not amplified and do not decay, while the transverse velocity oscillations increase gradually and reach, in amplitude, fairly large values (almost 60% of the incoming-flow velocity).

The transient process is completed when the regime of self-oscillations of the flow around the cylinder is established (Fig. 4b and d). This means that all the integral and local characteristics of the flow around the body represent near-sinusoidal time dependences. On the other hand, it is known that a Kármán vortex street is formed in the wake downstream of the cylinder; it is easily visualized at small velocities of the flow, e.g., by a smoke jet [18]. It follows from Fig. 5 that vortices execute a cyclic transverse motion from the upper and lower halves of the cylinder and displace simultaneously to the region of the wake. The Kármán vortex street arising at any distance from the cylinder represents a sequence of positive-vorticity and negative-vorticity zones, corresponding to absolute values of the vorticity of 0.5 and 1, with bunches of isolines located at their centers. The positions of the vorticity bunches correspond to the positions of the smoke-concentration cores calculated using the FLUENT package and the cores presented on the photograph of a flow visualized by smoke at Re = 140, taken from the Van-Dyke atlas [18]. The trajectory of a fluid particle, moving from the separation region to the cylinder, passes through the centers of the bunches and/or concentration cores and has a wave-like shape.

Fig. 5. Comparison of the smoke concentrations (a) measured (1) and calculated using the FLUENT package (2) and of the smoke concentrations (1) and the vorticity (3) calculated using the VP2/3 package (b) at Re = 140; the fields of vorticity isolines correspond to −5, −2.5, −1, −0.5, −0.1, −0.01, 0.01, 0.1, 0.5, 1, 2.5, and 5; b) trajectory of fluid particles moving in the neighborhood of the site of separation of the flow from the cylinder (4); data 1 were taken from the Van Dyke atlas [18].

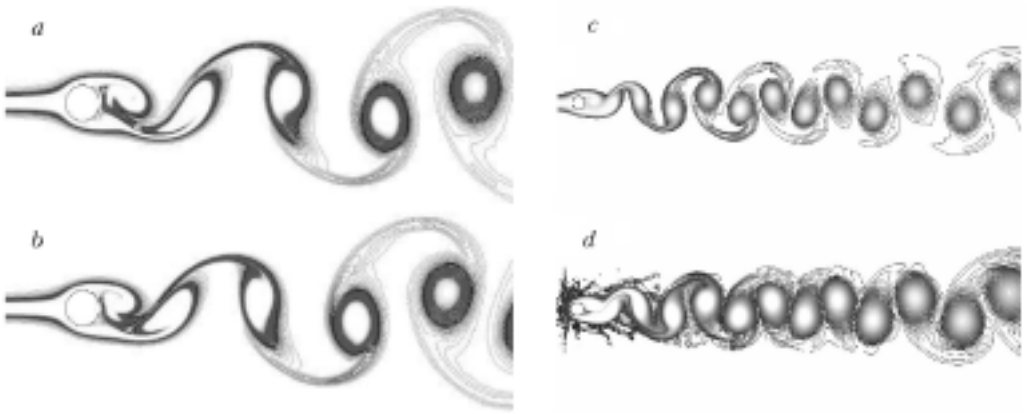

Fig. 6. Fields of concentrations (a, c) and vorticity (b, d) which are calculated using the FLUENT package and correspond to one and the same instant of time and different scales at Re = 140.

Table 1 presents pulsation force characteristics calculated for the period of oscillations of C_y. It is evident that the pulsations of the drag C_x' calculated with the use of different multiblock grids are in good agreement.

It was noted in [7] that an unsteady flow in the near wake downstream of a cylinder differs substantially from the fluid motion in a Kármán vortex street. Shear layers, characterized by a high level of vorticity, are developed with time, at first, in the upper half-plane and then, after a half-period of oscillations of C_y, in the lower half-plane. Vortex shrouds roll up into bunches, moving away from the body. The maximum, in magnitude, negative value of C_y is attained at the instant a developed upper large-scale vortex separates from the cylinder and, accordingly, the maximum positive value of C_y is attained when a lower large-scale vortex separates. The back of the body is constantly under the action of a fairly intense (velocity about 0.3) jet counter flow moving cyclically up-down about the geometric plane of symmetry.

The large-scale vortex structures coming down alternately are carried out downstream, and the thickness of the near wake increases rapidly and approximately proportionally to the distance from the cylinder (Figs. 5 and 6). In this case, the calculated rate of increase in the thickness of the wake correlates with the experimental one. In the far wake, the thickness of the layer in which a Kármán vortex street develops increases insignificantly and the synchronization of the vorticity and concentration cores is retained. It is also significant (Fig. 4e) that the Strouhal numbers calculated using different grids at Re = 140 are in good agreement with the values of Sh(Re) calculated and measured in [20, 28–32].

A fairly satisfactory agreement of the numerical forecasts obtained with the use of different grids and solvers with the available experimental data indicates, first of all, that the computational methods developed for solving the Navier–Stokes equations are adequate and the application program packages of different complexity, VP2/3 and FLUENT, are acceptable. Algorithms realized on nonstructured grids adapted to a solution and multiblock computational technologies based on structural intersecting grids are undoubtedly preferable directions of computational hydrodynamics that in all probability, should be combined in perspective.

Calculation of an Unsteady Turbulent Flow around a Circular Cylinder. A mathematical model based on a system of nonstationary Reynolds equations written in generalized curvilinear coordinates is used for solving the problem on a two-dimensional unsteady turbulent flow of an incompressible viscous fluid around a circular cylinder. The indicated equations are closed using the model of shear-stress transfer, which was used to advantage for calculating typical near-wall flows, including separation flows [5], and the one-parameter model of vortex viscosity SA [4].

The two-layer, low-Reynolds k–ω Menter model comprises the low-Reynolds, k–ω Saffman–Wilcox model (near the wall) and the standard k–ε Launder–Spalding model (in the outer zone). Thus, instead of the near-wall functions, with which high-Reynolds k–ε models are usually supplemented and which are not entirely correct mainly in the neighborhood of critical points, a flow in the layer adjacent to a wall is calculated using one of the best near-wall models. At a large distance from the wall, the solution is united with a k–ε model that is undoubtedly preferable for representation of shear layers. In this case, any additional terms are not introduced into the system of master equations for the characteristics of turbulence.

An important distinctive property of the k–ω Menter model is the use of the concept of shear-stress transfer, realized advantageously in the Johnson–King model [7]. The expression for the vortex viscosity in the initial variant of the Menter model involves the vorticity modulus. It is proposed in [33] to use, instead of this modulus, the strain-rate-tensor modulus. This modification of the Menter model is used in the present work, even through the difference between the estimates that were made using the new and initial variants of the Menter model is small.

The SA model is a one-parameter model with one differential equation for the vortex viscosity, in which the calculation of the length scale related to the local thickness of a shear layer is not necessary. The model was specially constructed for aerocosmic investigations and for estimation of the characteristics of near-wall flows. It showed itself to advantage in calculating boundary layers with a positive pressure gradient and when it was applied to turbomachines. The original SA model represents a low-Reynolds model that calls for a proper representation of the near-wall zone of a boundary layer. In the FLUENT package, the SA model is used in combination with near-wall functions when calculations are performed on relatively coarse grids. Note that the gradients of a transferable variable in the SA model are much smaller than the corresponding gradients for the k–ω and k–ε models, which makes the SA model less sensitive to numerical errors when nonstructured grids are used near walls. The model is not entirely faultless; in particular, it cannot predict the decay of a homogeneous isotropic turbulence.

It is significant that the standard SA model is used by default in the FLUENT package, while the preliminary investigations [34] have shown that a corrected SA model accounting for the significant influence of a correction on the difference of the strain-rate-tensor modulus from the vorticity modulus is preferable for calculating separation flows. In the present investigation, we used a corrected variant of the SA model.

The problem is formulated in a traditional way (see, e.g., [7]). A flow is undisturbed at the input outer boundary of the computational region. The characteristics of turbulence are formed in the same manner as in [7, 15] and correspond to the conditions of physical experiments performed in wind tunnels. For example, the energy of turbulence at the input boundary k_∞ is determined by the turbulence of the incoming flow (Tu_∞ = 1.5%) and the scale of turbulence L_∞ is of the order of D.

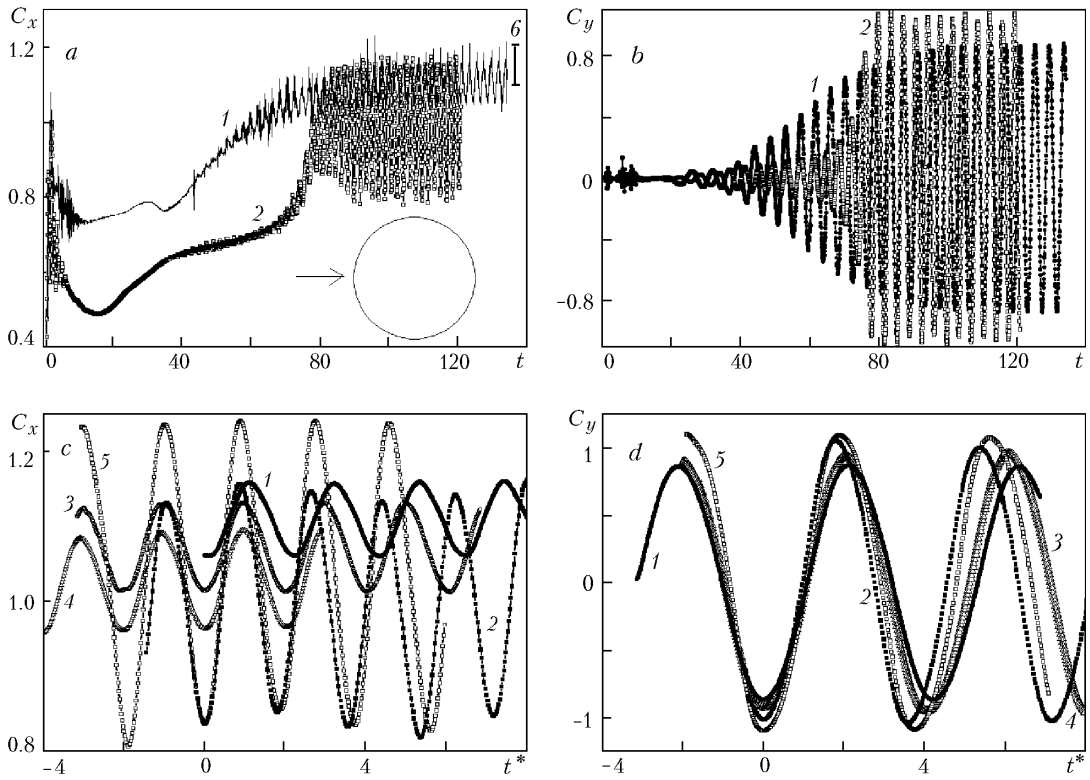

Fig. 7. Comparison of the processes of development of self-oscillations of C_x (a) and C_y (b) in a turbulent (Re = $4.5 \cdot 10^4$) flow around a circular cylinder and analysis of the influence of the turbulence modulus and the type of grids on the oscillations of C_x (c) and C_y (d): 1, 2) VP2; 3–5) FLUENT; 6) experiment [35, 36]; 1, 3, 4) MSST; 2, 5) SA; 1, 2, 3, 5) structured grids; 4) nonstructured grids.

Soft boundary conditions are set at the output outer boundary (solution is continued on condition that the second derivative of the dependent variable with respect to the coordinate normal to the boundary is equal to zero) and adhesion conditions are set on the surface of the body. At the side boundaries, soft boundary conditions are set when the VP2/3 package is used and the symmetry conditions are set when the FLUENT package is used.

The problem on the interaction of a uniform flow of an incompressible viscous fluid with a circular cylinder is solved beginning with the instant the cylinder is suddenly decelerated relative to the moving fluid. As a result, at the initial of time $t = 0$, the fluid strikes the body; in this case, all the parameters of the flow and the characteristics of turbulence in the computational region take input values.

Systematic calculations of a turbulent flow around a circular cylinder in an unlimited space are performed on a multiblock computational grid similar to the grid presented in Fig. 1d and e. This grid comprises three ring grids with a different concentration of nodes distributed uniformly along the peripheral coordinate, forming a fairly coarse external rectangular grid, and an additional very fine rectangular grid covering the wake. The first ring region of thickness 0.2 is covered by a 25×160 grid with a minimum step of 0.0005 near the wall (y^+ is smaller than 1 in a near-wall node). The second ring region of thickness 2 is covered by a grid with 40×100 cells. The outer rectangular region of size 49×34 is covered by a 170×120 grid with a minimum step of 0.1 in the longitudinal and transverse directions. In this case, the center of the cylinder is at equal distances from the lower and upper boundaries and at a distance of 17 calibers from the input left boundary. For better representation of the flow and the heat exchange in the wake, an additional grid containing 275×80 cells with a minimum step of 0.05 along the longitudinal and transverse coordinate is used. It covers a subregion of size 27.5×5.6 located at a distance of 0.3 from the cylinder.

For comparative analysis of the influence of the type of grid on the solution of a problem, we solved the problem on an unbounded, unsteady turbulent flow around a cylinder on a two-stage cylindrical grid similar to the

grid presented in Fig. 1b [7]. The ring zone of size 0.1, nearest to the cylinder, is covered by a 13 × 400 grid that is uniform along the peripheral coordinate and bunching toward the wall. The near-wall pitch is taken to be equal to 0.001. The outer ring region of radius 10 includes 200 × 400 cells.

To estimate the influence of a nonstationary factor on the solution of a problem, we calculated a steady turbulent flow in the half-plane of half the cylinder; this flow is similar, according to [10], to the flow around a cylinder with a separating plate. A multiblock computational grid contains three ring stages and an additional rectangular grid covering the wake. The first stage, containing 80 × 120 cells with a near-wall step of 10^{-4}, covers a region of width 0.5 adjacent to the cylinder. The second stage, containing 60 × 80 cells, covers a region of width 7 and the third stage, containing 20 × 80 cells, covers a region of width 35. A 140 × 40 grid covers a rectangular region of size 11 × 1 in the wake, located at a distance of 0.05 downstream of the semicylinder.

A turbulent flow around a circular cylinder was calculated using the FLUENT package on several structured and nonstructured grids similar to the grids presented in Fig. 2.

Figure 7 presents results of methodical calculations of the vortex dynamics of a turbulent subcritical flow around a circular cylinder. In addition to the presented integral and local characteristics, calculated on a set of intersecting Cartesian and cylindrical grids with the use of the VP2/3 package, we determined the characteristics of an unbounded two-dimensional flow around a transversal cylinder within the framework of the FLUENT package. Moreover, to estimate the influence of the nonstationary factor on the solution of a problem, a steady flow corresponding to the flow around a cylinder with a separating plate installed in the wake was numerically simulated.

The results presented illustrate, first of all, the time process of formation of a vortex flow around a cylinder (Fig. 7a and b), measured beginning with the instant the flow strikes the body, as well as the behavior of the drag coefficients and the transverse force in the self-oscillation regime of flow (Fig. 7c and d) for the reduced time t^*, measured beginning with the instant at which $C_y = C_{y\min}$.

The calculation data on an unsteady turbulent flow around a circular cylinder, presented in Fig. 7, were obtained with the use of different multiblock structured and nonstructured grids on the basis of the specialized and universal packages of application programs. Analysis of these data has shown that they are in wholly satisfactory agreement with each other and with the available experimental data of [35, 36]. The data obtained indicate that the MSST and SA models can be used for determining the characteristics of unsteady separation flows and that the simplified two-dimensional approach can be used for calculating three-dimensional unsteady vortex flows in the wake downstream of a body. However, the scatter in the pulsations of the drag coefficient was very large, especially in the case where the SA model was used.

The evolution of a subcritical unsteady turbulent flow around a circular cylinder has much in common with the development of a laminar vortex flow of a viscous incompressible fluid near the body considered. The analogy of the characteristic features of these processes is explained by the fact that the field of a variable vortex viscosity corresponds in its maximum values to the local Reynolds numbers characteristic of a laminar flow (of the order of 10^2).

As was noted in [7], a turbulent flow around a body is impact in character at the initial stage of its development and has rapidly changing parameters and integral characteristics. The drag of the cylinder decreases sharply and, in this regime of flow around it, differs insignificantly from the potential one.

The next phase of the process is characterized by the formation and gradual development of a symmetric separation zone in the wake downstream of the cylinder. The length of the zone increases from zero to several diameters (approximately at t of the order of 20). In this case, the drag of the body continues to decrease monotonically and gradually approaches the value of C_x characteristic of a steady flow around a semicylinder, calculated for symmetric boundary conditions. It should be noted that the numerical forecast of this characteristic is in good agreement with the experimental data of [35], obtained for a cylinder with a separating plate in the wake.

The asymmetry of the separation zone in the wake downstream of the body is due to the instability developed in the far wake. As in the case of the laminar regime of flow (see, e.g., [7]), this phase, called the transient phase, can be divided into three periods. In the first of them, whose duration is of the order of 40, an instability in the wake does not cause marked changes in the aerodynamic coefficients of the circular cylinder. In the second period of the transient phase, the drag increases rapidly simultaneously with the oscillations of the transverse force but remains monotonic. At this stage, the pulsations in the wake downstream of the body increase and the separation zone decreases substantially. The third stage of the transient phase is characterized by the development of oscillations of the

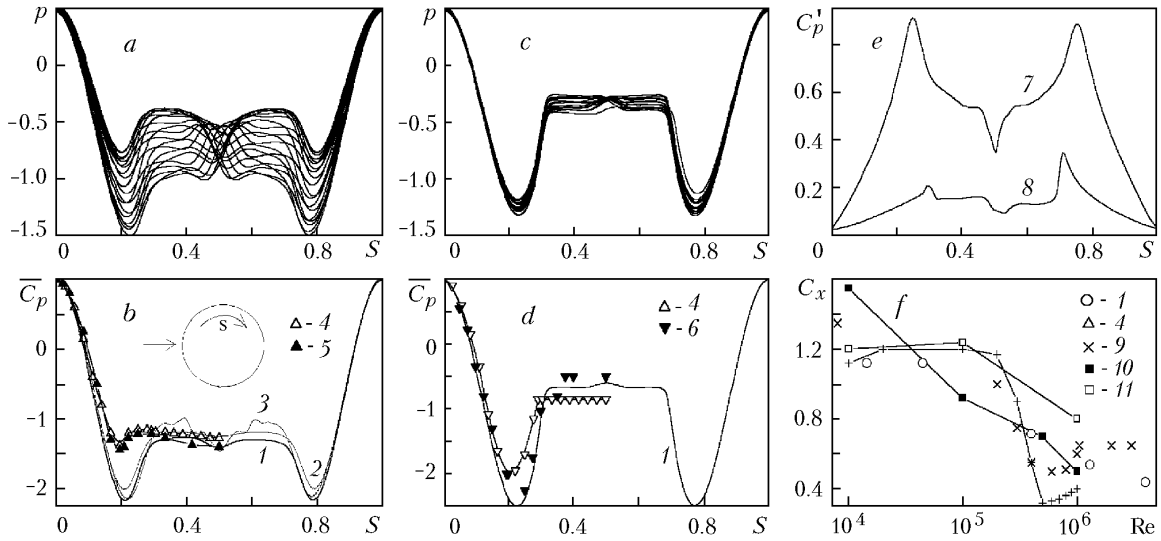

Fig. 8. Comparison of the instantaneous static-pressure distributions over the profile of a cylinder (a, c) superimposed in the period of C_y oscillations and of the averaged (b, d) and pulsating (e) components of the pressure coefficients in the subcritical (a, b, 7 — Re = $4.5 \cdot 10^4$) and supercritical (c, d, 8 — Re = $4 \cdot 10^6$) regimes of turbulent flow around the cylinder calculated using the VP2 and MSST packages (curves 1); curves 2 and 3 were obtained using the FLUENT package and the MSST and SA models; b, d) experimental data: 4) [35]; 5) [36]; 6) [37]; f) calculated (curve 1) and experimental dependences of C_x on Re: 4) [35], 90 [38], 10) [39], 11) [40]. Here, the sign of averaging is omitted.

frontal resistance, the amplitude of which gradually increases along with increase in the average value of C_x. The amplitude of the transverse-force oscillations becomes equal in order of magnitude to the drag force acting on the cylinder (Fig. 7b). At the final stage of the transient process, there arise oscillations not only in the wake but also upstream of the body. Eventually, all the characteristics of the flow becomes self-oscillating, i.e., they change periodically.

The oscillations of C_x and C_y in the regime of self-oscillations, presented in Fig. 7c and d, are somewhat different; however, the value of this difference can be considered as wholly acceptable and is easily explained by the use of different grids.

Figure 8 compares the calculation and experimental data on the local, integral, averaged, and pulsating characteristics of subcritical and supercritical flows around a circular cylinder at Reynolds numbers of $4.5 \cdot 10^4$ and $4 \cdot 10^6$. Analysis of the local and integral force characteristics was performed for the transverse-force oscillation period that is usually associated with the Strouhal number at which vortices are formed. The superposition of instantaneous pressure profiles, expressed in terms of the doubled kinetic head, in the period of oscillations of C_y (Fig. 8a and c) illustrates the zones of pressure oscillations. It should be noted that this period is divided into 19 time intervals, i.e., 20 curves are presented in each graph. One of the most interesting results of our calculations is determination of the boundaries of the zones of oscillations of parameters. It is evident that the regions filled partially with calculated profiles should be completely shaded when the degree of division of the period is increased. This means that the characteristics can be estimated from the probability positions, i.e., to any point of the profile of a body corresponds, with a statistical straggling, any average prognostic level. Broadly speaking, an analogy with experimental measurements of the static pressure suggests itself. Despite the fact that a flow around a cylinder is unsteady, the measured surface characteristics are, as a rule, independent of the time and correspond to average values, as follows, e.g., from Fig. 8b and d and from the experimental data of [35–37]. It should be noted that the average characteristics are determined as the mathematical expectation of the above-indicated profiles constructed with a constant time step in the period of oscillations of C_y. However, the averaged values can be estimated in a different way. At first, the coordinates of the upper and lower generating lines of the zone of oscillations of the instantaneous characteristics are determined, $f_{\max}$ and $f_{\min}$, and then

the average values are determined as $\bar{f} = (f_{max} + f_{min})/2$. The pulsating characteristics at the space points are determined as $f' = (f_{max} - f_{min})/2$.

Analysis of the surface distributions of the instantaneous characteristics (see Fig. 8a and c) has shown that their pulsations are largest in the separation zone, while in the regions of continuous flow without separation the oscillations are much smaller (by an order of magnitude), even though they are fairly large.

It should be noted that the calculated distributions of the average pressure coefficients over the profile of the cylinder differ somewhat from the measured ones (Fig. 8b). A somewhat higher, as compared to that in [35, 36], level of rarefaction in the zones of separation flow on the side surface, is equally well represented by the VP2/3 and FLUENT packages on different grids and on the basis of turbulence models of different complexity. At the same time, the estimated level of the bottom pressure is in good agreement with the experimental one.

For the supercritical regime of flow around a cylinder, the results of numerical calculations on the basis of the VP2/3 package with the use of the model of shear-stress transfer wholly satisfactorily correspond to the measurement data of [37, 38] (Fig. 8d).

As follows from Fig. 8e, the pulsations of the static-pressure coefficient in the subcritical regime of flow are four times larger than the analogous pulsations in the supercritical regime. Evidently, this is due to the substantial decrease in the sizes and intensity of the separation zone in the near wake.

Comparison of the experimental and calculated dependences of the drag coefficient of the circular cylinder on the Reynolds number has shown that the numerical forecasts made on the basis of the VP2/3 package with the use of the model of shear-stress transfer are wholly satisfactory, even though they do not reproduce a jump-like increase in C_x with increase in Re. However, no one computational method, including the LES model of large vortices, can reproduce the decrease in C_x.

Conclusions. Comparison of the numerical estimates made in solving the problem on an unsteady two-dimensional flow around a circular cylinder with the use of the VP2/3 and FLUENT program packages and the MSST and SA semiempirical differential models of turbulence, which are most frequently used in engineering practice, has shown that they are close and are practically independent of the grid used. The calculated integral and local characteristics of the flow investigated in the subcritical and supercritical regimes, correlate, on the whole, well with the experimental ones, which points to the fact that the indicated packages can be used for calculating unsteady separation flows and the simplified quasi-two-dimensional approach can be used for numerical representation of a three-dimensional vortex flow in a wake.

This work was carried out with financial support from the Russian Basic Research Foundation (projects 04-02-81005, 05-02-16184, and 05-01-00162).

NOTATION

C_x and C_y, coefficients of frontal resistance and transverse force related to the kinetic head $\rho U^2/2$; C_p, coefficient of static pressure related to the kinetic head $\rho U^2/2$; D, diameter of the cylinder, m; f, arbitrary variable; $\bar{f}$ and f', pulsating components of f averaged over the period T; k, energy of turbulence related to U^2; L, scale of turbulence related to D; p, pressure related to the doubled kinetic head ρU^2; Re, Reynolds number, $\mathrm{Re} = UL/\nu$; S, relative length along the cylinder profile measured from the frontal critical point; Sh, Strouhal number, $\mathrm{Sh} = 1/T$; T, oscillation period of C_y related to D/U; t, time related to D/U; Tu, degree of turbulence (related to U); U, velocity of a uniform flow, m/sec; u and v, horizontal and vertical coordinates related to D; y^+, dimensionless distance from the wall; Y, mass fraction; ε, rate of dissipation of the turbulence energy related to U^3/D; μ, coefficient of dynamic viscosity, kg/(m·sec); ν, kinematic viscosity, m^2/sec; ρ, density, kg/m^3; ω, specific rate of dissipation of the turbulence energy related to U/D; $|\,|$, absolute value. Subscripts: max and min, maximum and minimum values; i, number of a component; ∞, value in an incoming flow.

REFERENCES

1. S. A. Isaev, I. A. Pyshnyi, A. Yu. Snegirev, A. E. Usachov, and V. B. Kharchenko, Multiblock computational technologies of solving fundamental, applied, and exploitation problems of power engineering and transport, in:

G. A. Kryzhanovskii and E. A. Kuklyov (Eds.), *Nauch. Vestn. Akad. Grazhd. Aviats.*, *Ser. Probl. Bezopasn. Poletov i Ékspluat. Vozdush. Transp.*, No. 1, 50–58 (2003).
2. S. A. Isaev, Development of multiblock computational technologies for solving the problems of vortex aeromechanics and thermal physics, in: *Proc. 14th School-Seminar of Young Scientists and Specialists guided by academician of Russian Academy of Sciences A. I. Leontiev "Problems of Gas Dynamics and Heat and Mass Transfer in Power Plants"* [in Russian], Vol. 1, MÉI, Moscow (2003), pp. 13–16.
3. Fluent Inc. Fluent 6.1 Users Guide, Lebanon (2003).
4. P. R. Spalart and S. R. Allmaras, *A One-Equation Turbulence Model for Aerodynamic Flows*, AIAA Paper, No. 92-0439 (1992).
5. F. R. Menter, *Zonal Two-Equation k–ω Turbulence Models for Aerodynamic Flows*, AIAA Paper, No. 93-2906 (1993).
6. A. D. Gosman, Developments in industrial computational fluid dynamics, *Trans. IChemE*, **76**, Pt. A, No. 2, 153–161 (1998).
7. A. V. Ermishin and S. A. Isaev (Eds.), *Control over a Flow Past Bodies with Vortex Cells as Applied to Flying Vehicles of Integral Arrangement* (*Numerical and Physical Modeling*) [in Russian], MGU, Moscow (2003).
8. S. A. Isaev, S. V. Guvernyuk, M. A. Zubin, and Yu. S. Prigorodov, Numerical and physical modeling of a low-velocity air flow in a channel with a circular vortex cell, *Inzh.-Fiz. Zh.*, **73**, No. 2, 346–353 (2000).
9. S. A. Isaev, P. A. Baranov, S. V. Guvernyuk, and M. A. Zubin, Numerical and physical modeling of turbulent flow in a divergent channel with a vortex cell, *Inzh.-Fiz. Zh.*, **75**, No. 2, 3–8 (2002).
10. S. A. Isaev, Yu. S. Prigorodov, and A. G. Sudakov, Numerical analysis of the efficiency of vortex cells in laminar and turbulent flows past a circular cylinder with built-in rotating bodies, *Izv. Ross. Akad. Nauk*, *Mekh. Zhidk. Gaza*, No. 4, 88–96 (2000).
11. P. A. Baranov, S. A. Isaev, A. I. Leont'ev, A. V. Mityakov, V. Yu. Mityakov, and S. Z. Sapozhnikov, Physical and numerical modeling of vortex heat transfer in turbulent flow past a spherical hole on a plane, *Teplofiz. Aéromekh.*, **9**, No. 4, 521–532 (2002).
12. P. A. Baranov, S. A. Isaev, N. A. Kudryavtsev, and V. B. Kharchenko, Calculation of oscillations of a cylindrical pendulum in a cavity filled with a viscous fluid with the use of sliding multiblock grids, *Inzh.-Fiz. Zh.*, **76**, No. 5, 61–70 (2003).
13. P. A. Baranov, A. D. Golikov, S. A. Isaev, G. M. Makhviladze, and A. Yu. Snegirev, Numerical and physical modelling of fire development and smoke movement in a subway tunnel, in: *Proc. Third Int. Seminar on Fire and Explosion Hazards*, 10–14 April 2000, Windermere, Lake District, UK (2001), pp. 745–757.
14. V. V. Babaskin, S. A. Isaev, Kh. T. Metov, and V. V. Chepiga, A system for warning about a dangerous shift of wind, *Vseros. Nauch.-Tekhn. Zh. "Polet*," **8**, 10–16 (2000).
15. I. A. Belov, S. A. Isaev, and V. A. Korobkov, *Problems and Methods of Calculation of Separating Flows of Incompressible Fluid* [in Russian], Sudostroenie, Leningrad (1989).
16. S. A. Isaev, V. L. Zhdanov, and H.-J. Niemann, Numerical study of the bleeding effect on the aerodynamic characteristics of a circular cylinder, *J. Wind Eng. Ind. Aerodyn.*, **90**, Issue 11, 1217–1226 (2002).
17. S. A. Isaev and A. I. Leont'ev, Numerical modeling of vortex intensification of heat transfer in turbulent flow past a spherical hole on the wall of a narrow channel, *Izv. Ross. Akad. Nauk*, *Teplofiz. Vys. Temp.*, **41**, No. 5, 755–770 (2003).
18. M. Van Dyke, *An Album of Fluid Motion* [Russian translation], Mir, Moscow (1986).
19. S. A. Isaev, A. I. Leont'ev, and A. E. Usachov, Methodological aspects of numerical simulation of the dynamics of vortex structures and heat transfer in viscous turbulent flows, *Izv. Ross. Akad. Nauk*, *Énergetika*, No. 4, 140–148 (1996).
20. P. A. Baranov, S. A. Isaev, and A. G. Sudakov, Numerical modeling of the effect of generated vorticity on the Kármán street downstream of a circular cylinder, *Izv. Ross. Akad. Nauk*, *Mekh. Zhidk. Gaza*, No. 2, 68–74 (2000).
21. V. L. Zhdanov, S. A. Isaev, and H.-J. Niemann, Control of the near wake downstream of a circular cylinder in blowing out of low-head jets, *Inzh.-Fiz. Zh.*, **74**, No. 5, 36–38 (2001).

22. S. A. Isaev, P. A. Baranov, N. A. Kudryavtsev, I. A. Pyshnyi, and V. B. Kharchenko, Numerical simulation of unsteady turbulent flow past a thick profile with vortex cells with suction from the surface of central bodies, *Aéromekh. Gaz. Dinam.*, No. 3, 3–15 (2002).
23. P. A. Baranov, V. L. Zhdanov, S. A. Isaev, V. B. Kharchenko, and A. E. Usachov, Numerical simulation of unsteady laminar flow past a circular cylinder with a perforated case, *Izv. Ross. Akad. Nauk*, *Mekh. Zhidk. Gaza*, No. 2, 44–55 (2003).
24. S. A. Isaev, A. G. Sudakov, P. A. Baranov, and N. A. Kudryavtsev, Testing of a multiblock algorithm of calculation of nonstationary laminar separating flows, *Inzh.-Fiz. Zh.*, **75**, No. 2, 28–35 (2002).
25. S. A. Isaev, A. G. Sudakov, A. E. Usachov, and V. B. Kharchenko, Calculation of nonstationary flow around a circular cylinder within the framework of multiblock computational technologies, *Inzh.-Fiz. Zh.*, **75**, No. 5, 115–121 (2002).
26. J. M. Weiss, J. P. Maruszewski, and W. A. Smith, Implicit solution of preconditioned Navier–Stokes equations using algebraic multigrids, *AIAA J.*, **37**, No. 1, 29–36 (1999).
27. J. H. Ferziger and M. Peric, *Computational Methods for Fluid Dynamics*, Heidelberg, Berlin (1999).
28. B.-K. Min and K.-S. Chang, A momentum coupling method for the unsteady incompressible Navier–Stokes equations on the staggered grid, *Int. J. Numer. Meth. Fluids*, **28**, No. 3, 443–460 (1998).
29. C. Norberg, An experimental investigation of the flow around a circular cylinder: Influence of aspect ratio, *J. Fluid Mech.*, **258**, 287–316 (1994).
30. C. H. K. Williamson and A. Roshko, Measurements of base pressure in the wake of a cylinder at low Reynolds numbers, *Z. Flugwissund. Weltraumforsch*, **14**, No. 1–2, 38–46 (1990).
31. C. H. K. Williamson, Oblique and parallel modes of vortex shedding in the wake of a circular cylinder at low Reynolds numbers, *J. Fluid Mech.*, **206**, 579–627 (1989).
32. P. G. Esposito, R. Verzicco, and P. Orlandi, Boundary condition influence on the flow around a circular cylinder, bluff-body wakes, dynamics and instabilities, in: H. Eckelmann, J. M. R. Graham, P. Huerre, and P. A. Monkewitz (Eds.), *Proc. IUTAN Symp.*, Springer-Verlag, Berlin (1992), pp. 47–50.
33. F. R. Menter, M. Kuntz, and R. Langtry, Ten years of industrial experience with the SST turbulence model, in: *Proc. Int. Conf. Turbulence: Heat and Mass Transfer 4*, Begell House, Inc. (2003), p. 8.
34. S. A. Isaev, N. A. Kudryavtsev, D. A. Lysenko, and A. E. Usachov, Retrospective analysis of semi-empirical differential models of turbulence for calculation of separating flows, in: *Proc. III Int. School-Seminar "Models and Methods of Aerodynamics"* [in Russian], Izd. MTsNMO, Moscow (2003), pp. 54–55.
35. A. Roshko, Experiments on the flow past a circular cylinder at very high Reynolds number, *J. Fluid Mech.*, **10**, 345–356 (1961).
36. T. Igarashi, Flow characteristics around a circular cylinder with slit, *Bull. JSME*, **21**, No. 154, 654–664 (1978).
37. N. M. Bychkov and V. V. Larichkin, *Pressure and Fluctuations on a Cylinder at Small Distances from a Screen* [in Russian], Report No. 1658 of the Institute of Theoretical and Applied Mechanics, NGR 81065679, ITPM SO AN SSSR, Novosibirsk (1986).
38. V. A. Gushchin and V. N. Kon'shin, *Nonstationary separating and transient liquid flows near bodies of finite size*, in: *Etudes on Turbulence* [in Russian], Nauka, Moscow (1994), pp. 259–274.
39. R. P. Selvam, M. J. Tarini, and A. Larsen, Three-dimensional simulation of flow around a circular cylinder using LES and FEM, in: *Proc. 2 EACWE*, Genova, Italy (1997), pp. 831–838.
40. T. Tamura, I. Ohta, and K. Kuwahara, On the reliability of two-dimensional simulation for unsteady flows around a cylinder-type structure, *J. Wind Eng. Ind. Aerodyn.*, **35**, 275–298 (1990).